Journal of Chromatography A 1666 (2022) 462836

Contents lists available at ScienceDirect

Journal of Chromatography A

journal homepage: www.elsevier.com/locate/chroma

Determination of xylooligosaccharides produced from enzymatic hydrolysis of beechwood xylan using high-performance anion-exchange chromatography tandem mass spectrometry

Estrella Sanz Rodríguez[a,b,*], Gloria Lizeth Díaz-Arenas[c,d,e], Stefan Makart[f], Debjani Ghosh[c,g], Antonio Frank Patti[c,g], Gil Garnier[c,d,e], Joanne Tanner[c,d,e], Brett Paull[a,b]

[a] Australian Centre for Research on Separation Science (ACROSS), School of Natural Sciences, University of Tasmania, GPO Box 252-75, Hobart, Tasmania 7001, Australia
[b] ARC Industrial Transformation Research Hub for Processing Advanced Lignocellulosics (PALS), School of Natural Sciences, University of Tasmania, Hobart, Tasmania 7001, Australia
[c] ARC Industrial Transformation Research Hub for Processing Advanced Lignocellulosics (PALS), Department of Chemical and Biological Engineering, Monash University, Clayton, Victoria 3800, Australia
[d] Bioresource Processing Research Institute of Australia (BioPRIA), Department of Chemical and Biological Engineering, Monash University, Clayton, Victoria 3800, Australia
[e] Department of Chemical and Biological Engineering, Monash University, Clayton, Victoria, Australia
[f] Thermo Fisher Scientific, 5 Caribbean Dr, Scoresby, Victoria 3179, Australia
[g] School of Chemistry, Monash University, Clayton, Victoria 3800, Australia

ARTICLE INFO

Article history:
Received 16 December 2021
Revised 14 January 2022
Accepted 18 January 2022
Available online 22 January 2022

Keywords:
High-performance anion-exchange chromatography
Mass spectrometry
Xylooligosaccharides
Beechwood xylan

ABSTRACT

High-performance anion-exchange chromatography (HPAEC) coupled with triple quadrupole mass spectrometry (HPAEC-QqQ-MS) was applied to the determination of xylooligosaccharides (XOS) derived from enzymatically hydrolysed commercial xylan from beechwood and the analytical performance and advantages of the method explored. Separation, eluent suppression, electrospray ionisation, and detection options to enhance XOS sensitivity and selectivity were evaluated, delivering a new simple, fast, selective, and sensitive solution for the characterisation of these complex compounds. The method was fully validated in terms of its analytical performance for those XOS for which standards were available, i.e., degree of polymerisation from 1 to 6. The new method was applied to the analysis of xylan hydrolysates obtained by different enzymatic hydrolysis treatments using endo-xylanase from *Thermomyces lanuginosus*, characterising 25 different XOS and demonstrating the method's utility for future tailoring of enzymatic hydrolysis conditions to obtain desired XOS profiles in such hydrolysates. Linear XOS and 4-*O*-methyl glucuronic acid (MeGluA) branched XOS were detected by direct injection of the xylan hydrolysates after a simple 10-fold sample dilution and filtration. Identification of XOS detected by HPAEC-QqQ-MS was additionally confirmed using high-resolution orbitrap mass spectrometry (HR-orbitrap-MS). Further, an ultra-sensitive and -selective method was developed by using selected reaction monitoring acquisition mode (SRM), increasing signal-to noise ratio and decreasing the limits of detection, opening future applications to low concentrated sample analysis.

1. Introduction

Xylooligosaccharides (XOS) are carbohydrate oligomers which are reported to offer multiple health benefits, such as strengthening the immune system, modulating intestinal microbiota and reducing the risk of cancer. Additionally, these valuable compounds exhibit high temperature and pH range stability and low-calorific value [1]. As a result, XOS have been integrated into several nutraceuticals, such as prebiotics, and have thus become a rapidly growing commodity in the actual health-food market [2,3]. According to 2021 Global Info Research (GIR) report, in 2020 the XOS market revenue was 102.1 Million USD, and is predicted to reach 135.7 Million USD in 2026, with a compound annual growth rate of 4.1% over 2021–2026 [4]. These sugars are found naturally in fruit, vegetables, bamboo shoots, honey and milk, albeit in small quanti-

* Corresponding author at: Australian Centre for Research on Separation Science (ACROSS), School of Natural Sciences, University of Tasmania, GPO Box 252-75, Hobart, Tasmania 7001, Australia.
E-mail address: estrella.sanzrodriguez@utas.edu.au (E. Sanz Rodríguez).

https://doi.org/10.1016/j.chroma.2022.462836
0021-9673/

ties [5]. However, XOS can also be produced from xylan, one of the major components of the most abundant agro-industrial residues available globally, i.e. lignocellulosic biomass (LCB) [6,7]. Therefore, XOS could be considered a green, 'value added' commodity, since their production may contribute to sustainable development and the circular economy [8].

LCB is principally built of three structures: cellulose (30–50%, w/w), hemicellulose (20–40%, w/w) and lignin (15–25%, w/w) [9]. Xylan is the major heteropolysaccharide of hemicellulose, being composed of a linear backbone of β-D- xylopyranosyl (xylose) residues linked by β-1,4-glycosidic bonds [2]. This backbone may be substituted with arabinose, 4-*O*-methyl glucuronic acid (MeGluA), ferulic acid, p-coumaric acid and/or acetyl side groups [10]. XOS production is based on the hydrolysis of xylan, which can be achieved by chemical, enzymatic or chemoenzymatic methods [5,11–19]. Depending upon various xylan sources and production methods used for XOS manufacture, the structure of the XOS obtained vary in degree of polymerisation (DP) and in degree and type of substitution [3,12]. The function of XOS is governed by their specific structure [18]. Considering the significance of structure-function relationships, there is currently considerable demand for reproducible, fast and simple analytical methods for characterisation and quantitation of manufactured XOS from LCB [10].

The advances in XOS characterisation during the last twenty years have been predominantly facilitated by the use of mass spectrometry (MS), specifically matrix-assisted laser desorption ionisation coupled to mass spectrometry (MALDI-MS) [11,13,14,16,20–31] and electrospray ionisation mass spectrometry (ESI-MS) [10,12,15,27,32–43]. The most common protocols for the structural characterisation of XOS reported within these previous methods have included a step where the hydrolysates from the LCB treatment are first fractionated, following by off-line analysis using a technique for structural characterisation, including nuclear magnetic resonance (NMR), and as mentioned above, MALDI-MS or ESI-MS [44]. Fractionation is often carried out by chromatographic techniques such as gel filtration chromatography (GFC) or size exclusion chromatography (SEC). In a few studies, a separation technique hyphenated with ESI-MS is reported, typically liquid chromatography, such as hydrophilic interaction liquid chromatography (HILIC) [33] or reversed-phase high performance liquid chromatography (RP-HPLC) [12,32,37].

An alternative approach using ion chromatography (IC), although referred to as 'high-performance anion-exchange chromatography' (HPAEC), was developed in the late 1980s, and when coupled with pulse amperometric detection (PAD), soon became the gold standard technique for the analysis of complex mixtures of carbohydrates due to its advantageous selectivity and sensitivity [45]. HPAEC can deliver highly selective separations of oligosaccharides when using a strong anion-exchange stationary phase, under high-pH conditions with a hydroxide-based eluent [46]. HPAEC-PAD has been successfully applied to the determination of XOS over a wide DP range, as reported within a large number of publications [12,13,15,16,23,30,35,41–43,47,48]. However, although the selectivity provided by HPAEC cannot currently be exceeded by any other separation technique, PAD detection, despite providing high sensitivity for XOS with DP from 2 to 12, remains incapable of providing structural confirmation, or detecting co-eluting XOS species, or indeed identifying unknown XOS species where standards are not available, which is an essential requirement when researching into enzymatically based XOS production processes.

Suppressed IC (or suppressed HPAEC), where the eluent is converted to pure water within a suppressor or desalter, offers a solution to allow HPAEC couple on-line with MS detection. There are clear advantages to coupling suppressed HPAEC and MS compared with standard PAD detection, most notably the ability to detect and quantify co-eluting species, and to confirm the identity of target solutes and unknowns, via their individual mass spectra. Although HPAEC-MS has been used in several studies for the determination of carbohydrates in different samples [49–51], and HPAEC has also been used for sample fractionation before off-line XOS analysis by MALDI-MS or ESI-MS [23], to the authors' knowledge, HPAEC has never been directly coupled to ESI-MS for XOS determination in complex treated biomass samples. However, interfacing HPAEC directly with MS presents several technical challenges particularly for this specific application, as elution of XOS with high DP requires higher ionic strength alkaline eluents than for other smaller carbohydrates. Specifically, incomplete salt removal by the suppressor/desalter can be problematic, which to-date has likely restricted attempts to directly couple of HPAEC with MS for XOS separation and characterisation.

Herein, for the first time, a HPAEC coupled to a triple quadrupole mass spectrometer (HPAEC-QqQ-MS) based method was applied for the determination of XOS derived from enzymatically treated xylan. Five enzymatic hydrolysis treatments using endo-xylanase from *Thermomyces lanuginosus* were applied to beechwood xylan characterising 25 XOS and demonstrating the method's utility for tailoring hydrolysis conditions to obtain desired XOS. Identification of XOS detected by HPAEC-QqQ-MS was further validated using high-resolution orbitrap mass spectrometry (HR-orbitrap-MS). Finally, an ultra-sensitive and -selective method, was also developed using selected reaction monitoring acquisition mode (SRM), substantially increasing signal-to noise ratio and decreasing the limits of detection.

2. Experimental

2.1. Chemicals and standards

De-ionised water (DIW) was obtained from a Millipore Milli-Q water purification system (Bedford, MA, USA). Individual 100 mg L^{-1} stock solutions of xylose (X1) from Sigma (purity 99%, St. Louis, MO, USA), and xylobiose (X2), xylotriose (X3), xylotetraose (X4), xylopentaose (X5) and xylohexaose (X6) from Megazyme Inc (purity > 95%, Chicago, IL, USA) were prepared by dissolving the appropriate amount of each XOS in DIW. Carbon-13-labelled levoglucosan (1,6-anhydro-β-D-glucopyranose (U-13C6), from Cambridge Isotope Laboratories Inc, purity 98% (Tewksbury, MA, USA), was used as an internal standard (IS). A stock solution of the IS was prepared by dissolving 0.05 g in 25 mL of DIW to produce a 2000 mg L^{-1} concentration.

Stock solutions of X1-X6 were used to prepare an intermediate solution containing a mixture of X1-X6. An internal standard calibration method was used to quantify targeted solutes. Working solutions to construct 6-point calibration curves were prepared daily by diluting the intermediate solution to concentration levels similar to those expected in samples, and adding a fixed amount of IS. After the proper dilutions, the IS concentration in the sample/standard analysed was constant at 20 mg L^{-1}. All stock and intermediate solutions were kept at 4 °C and stored in polypropylene containers until use.

Extra pure sodium hydroxide (NaOH) 50% (w/w) solution in water, and electrochemical-grade sodium acetate salt (NaOAc) (preweighed reagent), both from Thermo Fisher Scientific (Sunnyvale, CA, USA), were used for the preparation of the HPAEC eluents. Methanol, (MeOH) from Honeywell Burdick & Jackson (Muskegon, MI, USA), and lithium chloride (LiCl) from Sigma-Aldrich, purity 99+% (St. Louis, MO, USA), were used to prepare the MS make-up solution. Xylan from beechwood (*Fagus sylvatica L.*), obtained from Apollo Scientific (Cheshire, UK), was used as substrate for enzymatic hydrolysis by endo-(1,4)-β-xylanase from *Thermomyces lanuginosus* (≥ 2500 U/g, Sigma-Aldrich, St Louis, USA). Citric

Table 1
Enzymatic hydrolysis conditions applied to produce samples analysed in this study.

Sample	Temp (°C)	pH	Reactor type
1	35	7.0	Incubator shaker
2	35	4.0	Incubator shaker
3	50	4.0	Incubator shaker
4	25	4.0	Continuous flow microfluidic reactor
5	25	5.0	Continuous flow microfluidic reactor

acid monohydrate and sodium citrate dihydrate, both from Sigma-Aldrich (St Louis, USA), were used to prepare the buffer solutions for the enzymatic hydrolyses.

2.2. Enzymatic hydrolysis of beechwood xylan

The enzymatic hydrolysis of beechwood xylan by endo-xylanase to produce XOS was conducted as follows: 2% (w/v) xylan and 62.5 U mL^{-1} enzyme were added to 10 mL of 50 mM sodium citrate buffers prepared at pH 4.0, 5.0 and 7.0. The mixtures were incubated at different temperatures (25, 35 and 50 °C) either on an incubator shaker or a continuous flow microfluidic reactor. The incubator shaker (Infors Ecotron) was set at 200 rpm for 40 min. Operational conditions by using the continuous flow microfluidic reactor are detailed elsewhere [52]. Table 1 details pH, temperature, and reactor type for the five enzymatic hydrolysis treatments (samples 1–5) applied in this study. After the reaction time was completed, the enzyme was denatured by heating the samples for 5 min in a water-bath at 100 °C following a protocol proposed by Ghosh et al. [52]. The resulting hydrolysates were centrifuged (Thermo Scientific Sorvall LYNX 4000) at 10,000 rpm and 20 °C for 10 min. The supernatant liquors were diluted x10 with DIW and filtered through a Nylon 0.22 µm syringe filter before their analysis by HPAEC-QqQ-MS.

2.3. Instrumental

A Thermo Scientific Dionex ICS-5000^{+} Reagent-Free IC (RFIC) system coupled to a Thermo Scientific TSQ Quantiva triple-stage quadrupole mass spectrometer, equipped with an Ion Max NG source operating in heated-ESI (H-ESI) mode, was used throughout. After sample dilution and filtration, 20 μL of sample was injected via an AS-AP autosampler (controlled temperature at 15 °C) onto a Dionex AminoTrap column (3 × 50 mm) and coupled CarboPac PA200 analytical column (3 × 250 mm). Target solutes were separated at 35 °C using a gradient from 2 to 150 mM of sodium acetate (NaOAc) over 30 min combined with a constant concentration of 150 mM of sodium hydroxide (NaOH) throughout. The flow rate was set at 0.450 mL min^{-1} within a total run time of 60 min, including a short cleaning step to elute strongly retained compounds and an equilibration step before the next injection. An anion self-regenerating Dionex ADRS 600 suppressor (4 mm) was placed in-line after the column, which electrolytically converted the NaOH eluent to water and NaOAc eluent to acetic acid. The suppressor was working in external-regenerating mode using an AXP pump to deliver DIW at 3 mL min^{-1}. The suppressor was automatically set at a current of 334 mA based on the eluent concentration and flow rate. A conductivity detector was installed after the suppressor, assisting in the evaluation of the efficiency of the suppression, providing a measurement of the background conductivity from acetic acid and remaining NaOH/NaOAc during the development of the method. Later, the conductivity detector was removed from the system to avoid any extra peak broadening. LiCl at a concentration of 0.5 mM in MeOH was added into the HPAEC eluate stream using a second auxiliary pump at a flow rate of 0.05 mL min^{-1}, via a mixing tee immediately before the divert valve to assist in ionisation at the ESI source and to enhance the signal of XOS via monitoring their positive lithium adducts. Detection was carried out in full-scan mode. All instrumentation, columns and suppressor were from Thermo Fisher Scientific (San Jose, CA, USA, USA). Instrument control, data acquisition and processing were via Chromeleon 7 Software, version 7.2.6 (10,049). A flow schematic of the HPAEC-QqQ-MS system used throughout is presented in Fig. 1 and a summary of the HPAEC-QqQ-MS instrumental parameters is presented in Table 2.

Identity of the compounds detected by HPAEC-QqQ-MS was confirmed using HR-Orbitrap-MS. Analyses were carried out using a hybrid LTQ Orbitrap XL mass spectrometer (Thermo Fisher Scientific, San Jose, CA, USA) housed at the Central Science Laboratory (University of Tasmania, Australia). The ESI source was set at positive ion mode with a capillary temperature of 350 °C, an ion spray voltage of 4 kV and a sheath gas flow rate of 8 (arbitrary units). Full-scan Fourier high resolution scanning range was 150–1800 *m/z* and resolution power of 30,000 FWHM. For MS/MS (MS^2) experiments, selected precursor ions were isolated in the LTQ ion trap, with a width of 2 Da and were fragmented using collision energies from 20 to 30 eV. Data were acquired and treated by means of Xcalibur Software, version 2.1.

2.4. Validation of the HPAEC-QqQ-MS method

Validation of the HPAEC-QqQ-MS method included evaluation of carry-over, limit of detection (LOD), limit of quantitation (LOQ), linearity and intra- and inter- day repeatability. Blank samples (DIW), along with zero samples (IS-spiked blank DIW) and pro-

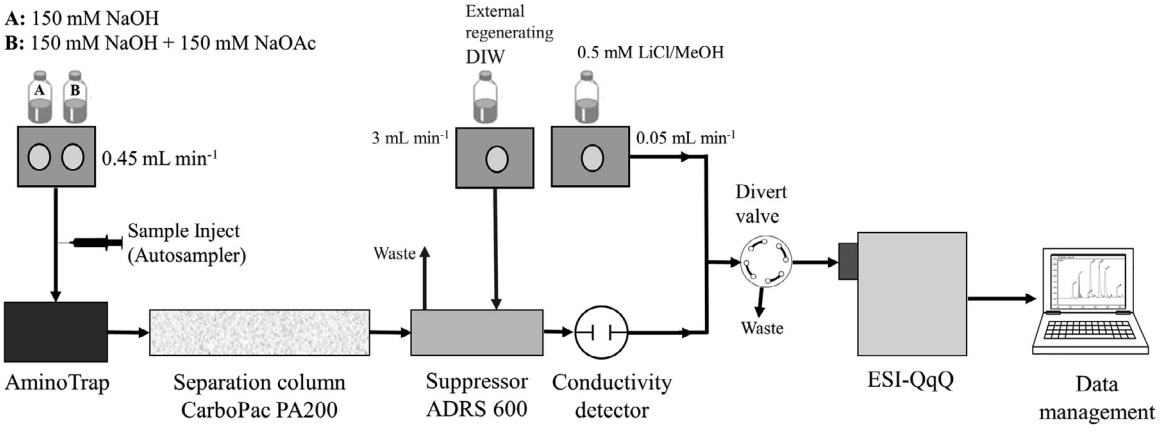

Fig. 1. Instrumental arrangement for the HPAEC-QqQ-MS system used in this study.

Table 2
HPAEC-QqQ-MS instrumental parameters and settings.

HPAEC	
Column:	CarboPac PA200 (3 × 250 mm), 5.5 μm
Guard:	AminoTrap (3 × 50 mm), 10 μm
Temperature:	35 °C
Injection volume:	20 μL
Eluent:	Gradient of NaOH/NaOAc in water
Eluent flow rate:	0.450 mL min^{-1}
Suppressor:	Dionex ADRS 600 (4 mm)
External Water Mode flow rate:	3 mL min^{-1}
Applied current:	334 mA
QqQ-MS	
Make-up solvent	0.5 mM LiCl in MeOH
Make-up solvent flow:	0.05 mL min^{-1}
Ion source Type:	H-ESI
Ionisation mode:	Positive
Spray voltage:	4500 V
Sheath gas:	55
Aux gas:	22
Sweep gas:	1
Ion transfer tube temp:	325 °C
Vaporiser temp:	350 °C
Acquisition mode	Full scan: *m/z* 50–1800 (50–1800 *m/z*) Scan rate (Da/s): 1000 Q1 Resolution (FWHM): 0.7
Acquisition mode	Selected reaction monitoring (SRM) Q1 Resolution (FWHM): 0.7 Q3 Resolution (FWHM): 0.7 CID Gas (mTorr): 1.5

Compound	Precursor (Q1) (*m/z*)	Product (Q3) (*m/z*)	Collision Energy (eV)	RF Lens (V)
X1	157	157	0	50
X2	289	289	0	93
X3	421	139	35.7	138
X4	553	139	46.3	248
X5	685	685	0	168
X6	817	817	0	197
IS	193	175	10	50

cedure blanks were analysed at the start of every analytical sequence to detect any possible contamination/interference coming from DIW, IS solution, injection vials, syringes, reagents and/or sample treatment vials. Blank samples injected after the highest calibration standards were used to determine carry-over issues. LODs and LOQs were determined at a signal-to-noise ratio (S/N) of 3 and 10, respectively. The number of data points used to define the linear range was six. Intra- and inter-day repeatability were determined over the same day and across four different weeks, respectively, from 10 replicates of a standard mixture containing 1 mg L^{-1} of X1, 20 mg L^{-1} of X2 and 0.5 mg L^{-1} of X3-X6.

3. Results and discussion

3.1. HPAEC-QqQ-MS method development

The development of the new method focused on four key-challenges: separation, eluent suppression, electrospray ionisation and detection.

3.1.1. Separation

HPAEC achieves highly selective separations of carbohydrates utilising a high pH stable pellicular anion-exchange column, high-pH eluent conditions (pH 12–14) and hydroxide-based eluents. Under these conditions, neutral and anionic carbohydrates are at least partially ionised and can be separated by predominantly anion-exchange interactions. The CarboPac PA200 column is a high-resolution strong anion-exchange column and it was developed for enhanced chromatography of oligosaccharides [53]. NaOH was used as eluent 'A', keeping a constant concentration to provide the necessary pH for retention, whilst simultaneously eluent 'B', NaOAc, was used in gradient mode to provide the 'competing ion' to facilitate elution of highly retained XOS. Different concentrations for both eluents and different gradients were tested to optimise the separation of a mixture of available standards, e.g., X1-X6. Baseline separation was achieved in less than 15 min using 150 mM NaOH (eluent A) and 150 mM NaOH/150 mM NaOAc (eluent B). The optimal gradient started at 2% B and ended at 51% B at 15 min. As XOS with higher DP, both linear and branched, were also expected in real samples, the gradient was extended up to 100% B at 30 min and kept constant for 10 min to allow for elution of more strongly retained XOS. Following this, at 45 min, the percentage of eluent B was reduced to initial conditions at 2% for 15 min to equilibrate the system before the next injection.

3.1.2. Eluent suppression

Concentrated NaOH and NaOAc eluents are incompatible with solute ionisation at the ESI source. However, the use of eluent suppressors within the IC systems has resolved this limitation for many IC applications. Suppressors in IC remove the eluent counter ions, together with sample counter-ions, and replace these with re-

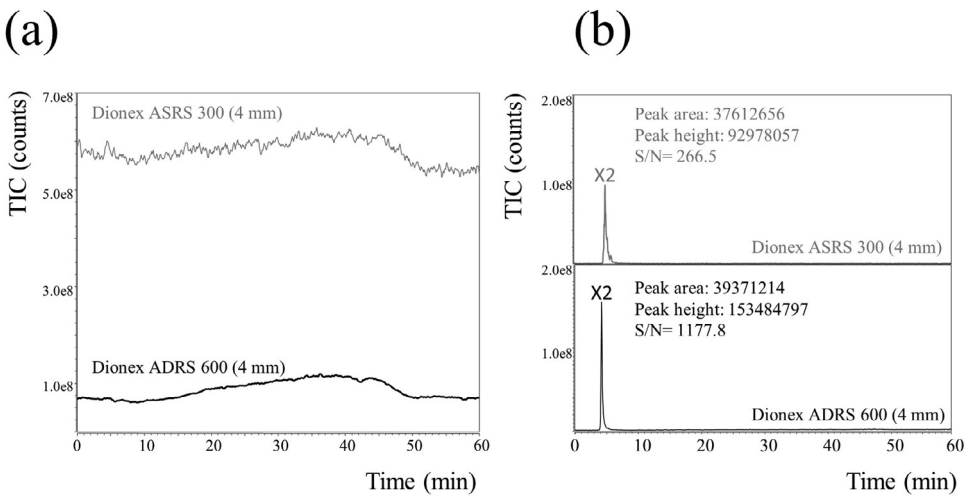

Fig. 2. (a) Total ion current (TIC) background signals using differing eluent suppressors (b) extracted ion chromatograms (EICs) for $[X2+Li]^+$ (*m/z* 289) obtained in the analysis of a standard mixture containing 20 mg L^{-1} of X2 using different eluent suppressors. Dionex ASRS 300 (4 mm) (grey line); Dionex ADRS 600 (4 mm) (black line).

generant ions, in doing so converting the eluent to either water (in the case of a NaOH eluent), or a weakly dissociating acid (e.g., acetic acid from acetate-based eluents) before entering the mass spectrometer.

To this end, two suppressors were evaluated in this study, namely a Dionex ASRS 300 (4 mm) and the latest Dionex ADRS 600 (4 mm) suppressor, both operating with DIW supplied externally at a flow rate of 3 mL min^{-1} as regenerant. Although, both suppressors offer high-capacity suppression and minimal dead volume added to the analytical system, the newer generation ADRS 600 contains improvements such as an ion exchange resin packed eluent chamber and serial regenerant flow, and is the only suppressor recommended and validated for neutralization mode for sample desalting. Indeed, the total ion current (TIC) background at the MS was reduced by a factor of 10 when using the ADRS 600 suppressor (Fig. 2(a)). Consequently, an increment of the signal-to-noise (S/N) ratio for X1-X6 in the range from 2.5 to 10-fold was achieved. As an example, Fig. 2(b) shows a comparison of the extracted ion chromatograms (EICs) at *m/z* 289, $[M+Li]^+$, for the analysis of a standard solution of X2 at 20 mg L^{-1} using both suppressors. The 4-fold improvement in the S/N observed for X2 when using the ADRS 600 suppressor can be attributed to a combination of a smaller dead volume added to the analytical system, providing improved peak shape, plus a reduction in the MS background from improved suppression. Results were similar or better for the rest of the standards tested, providing excellent S/N ratios and demonstrating that the capacity of the new ADRS 600 suppressor was appropriate for this specific application, where highly concentrated NaOH and NaOAc eluents were used.

3.1.3. Electrospray ionisation

Following efficient eluent desalting using the new ADRS 600 suppressor, efficient electrospray ionisation of complex structures of XOS, with increasing DP and branching, remains a challenge. The characterisation of complex oligosaccharides in off-line desalted samples by MS has been mainly carried out by MALDI-MS and ESI-MS in positive mode [54]. Saccharides predominantly form sodium adduct ions, detected with values in the range of *m/z* 100–1500 by ESI and over *m/z* 500 by MALDI, as lower *m/z* are impacted in MALDI-MS by matrix ion interferences [39]. In our previous study [50] we have demonstrated that lithium cationisation of anhydro monosaccharides using LiCl in the MeOH make-up solvent for ESI provided an increase in response of 100-fold for these solutes, compared with negative ESI, and an increase of 10-fold compared with sodium cationisation. Based on those results, positive lithium cationisation was chosen as optimal ionisation mode and similar conditions to those applied in our previous study were applied. The optimal make-up solvent flow rate was found to be 0.05 mL min^{-1} and the concentration of the make-up solvent lithium additive was set at the same value as than in our previous study, i.e., 0.5 mM, since it was found that higher concentrations of LiCl (1 and 2.5 mM) provided significantly lower responses to all carbohydrates tested, likely due to competitive ionisation suppression [50]. To our knowledge, this is the first-time lithium cationisation have been effectively used to detect XOS using ESI-MS. Other parameters at the ESI source, such as flow rate gases, ion transfer tube and vaporiser temperatures, are mainly flow-rate-dependant parameters. Therefore, optimal values were set for an incoming flow rate of 0.500 mL min^{-1}. A capillary voltage of 3.5 kV was selected based on both analysis of available standards and previous studies of higher XOS by ESI-MS [10,33,40].

3.1.4. Detection

In beech hardwood, xylan is made up of a core backbone of xylose units linked by $\beta-1,4$ bonds, which are mainly substituted with *O*-acetyl-4-*O*-methylglucuronic acid [14]. A disadvantage of performing HPAEC separations is that by using eluents with a high pH, alkali-labile esters such as *O*-acetyl will be removed [44]. Based on the literature, after an enzymatic hydrolysis treatment of beechwood xylan by endoxylanases from glycosyl hydrolase family GH11, such as *Thermomyces lanuginosus* used in this study [28,41], neutral XOS and 4-*O*-methylglucuronic acid (MeGluA) derivatives with DP from 1 to 16 could be present within the samples analysed herein. However, even though the expected compounds were known, the composition of the samples was unclear. Moreover, the new method developed aimed to be used in future studies for the analysis of XOS from different biomass sources, not only from beechwood xylan. Therefore, a full-scan acquisition method, across a wide range of *m/z* 100–1800, covering the expected *m/z* values for lithium species generated at the ESI source, was performed for the analysis of the hydrolysate samples, as detailed in Table 1. The analysis of the standards X1-X6 confirmed that the main species generated for all of them was $[M+Li]^+$, although $[M+H_2O+Li]^+$, $[M+CH_3OH+Li]^+$ and $[M+CH_3COOH+Li]^+$ were also observed for the standards tested as *m/z* increments from $[M+Li]^+$ of 18, 32 and 42 Da, respectively. Methanol adducts and acetic acid adducts were also seen due to the presence of methanol in the make-up solvent and acetic acid generated by suppression from NaOAc.

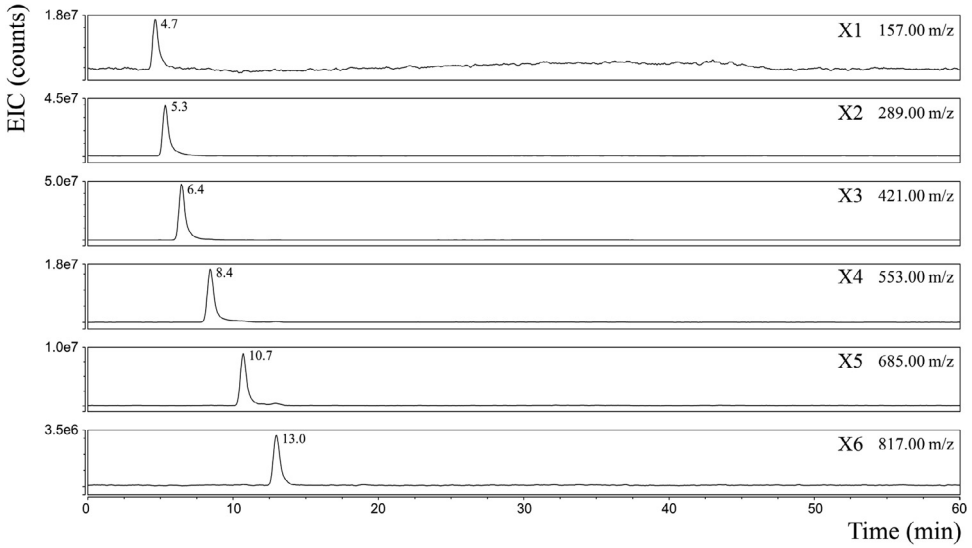

Fig. 3. Extracted ion chromatograms (EICs) obtained for the analysis of a standard mixture containing 4 mg L^{-1} of X1 -X6 using the optimal HPAEC-QQQ-MS developed.

Fig. 3 shows the EICs obtained for the analysis of a standard mixture containing 4 mg L^{-1} of X1-X6 using the new HPAEC-QqQ-MS method. It was observed that, at the same concentration, the MS response was similar for X2 and X3 but decreased as the mass of the xylooligosaccharide increased, e.g., the response for X3 was an average of 12.7 times higher than for X6 when different concentration levels were tested, confirming what previous studies had already observed, i.e., that ESI sensitivity decreases as the mass of the polysaccharide increases [55]. Therefore, poorer ionisation efficiency was expected for XOS with DP > 6, likely present in the real samples. Due to the high XOS concentration expected in the hydrolysates for some targeted solutes, to achieve a compromise between protection of the chromatographic column/detector and suitable sensitivity for those solutes presenting lower concentration/providing lower response, different sample dilution factors were also tested, and a 10-fold dilution factor was found to be optimal. Additionally, the poorer response observed for X1 could be due to a combination of chromatographic behaviour, since the CarboPac PA200 column used in this study is recommended for oligosaccharide profiling, not for monosaccharide analysis (poor retention and co-elution with unretained ions), and due to its low *m/z*, where most background ions are also present and can interfere in the detection.

3.2. Analytical performances of the HPAEC-QqQ-MS instrumental method

The proposed method was evaluated in terms of its analytical performance characteristics, such as LOD, LOQ, linear range and intra- and inter-day repeatability. These values are summarised in Table 3. Quantitation was carried out using an IS calibration method to correct for possible instrumental fluctuations. As shown in Table 3, the LODs for X3-X6 were from 0.003 to 0.059 mg L^{-1} using full-scan mode. These are by far the lowest LODs reported in the literature for the quantitation of X3-X6 from LCB hydrolysates to-date. LODs for X1 (0.311 mg L^{-1}) and X2 (0.003 mg L^{-1}) are similar to those reported before for other studies [56,57]. The LOD for X1 was slightly higher than for the rest of the standards tested for reasons discussed above. HPAEC-PAD has typically been applied for the quantitation of X1-X6 in LCB hydrolysates and the literature cited in Table 3 are examples of those quantitative studies. However, to our knowledge, a validated method for the quantitation of X1-X6 using MS has not been presented in the literature to-date, highlighting the significance of the present study which is able to simultaneously quantify and confirm the XOS identify. No significant background XOS concentration were observed in blank samples (DIW), IS-blank samples or procedure blank samples. No carry-over issues were identified for blank samples injected after the highest calibration point. Six-point calibration data for X1-X6 were found to fit a linear equation with regression coefficients (R^2) higher than 0.995 for all XOS, with the specific upper limits of the linear range tested for each XOS detailed in Table 3. Upper limits of the linear range were set to cover the possible range of sample concentrations of each saccharide in the real samples. It can be also observed from Table 3 that intra-day repeatability was typically below 5.3% for quantitation values of interest. Inter-day repeatability values were under 12.0% for X2 and X3 but they were higher for X1 and X4-X6, up to 24.3%, due to the concentration in the test mixture for those solutes being close to their LOQ. Regardless, all %RSD were within acceptable values for the concentration levels tested [58].

3.3. Analysis of xylan hydrolysates by HPAEC-QqQ-MS

To evaluate the applicability of the method developed, five hydrolysates obtained following different enzymatic treatments detailed in Table 1 were analysed. The main objective was to determine the enzymatic hydrolysis products obtained by different enzymatic hydrolysis methods. Amongst the approaches to produce XOS from LCB, enzymatic hydrolysis was recently highlighted due to the enzyme specificity and the mild reaction conditions required [59]. Applications of XOS are determined by their DP, and type and number of substituents. Low DP XOS (X2-X4) have potential to be used as prebiotics and anti-microbial and anti-inflammatory agents, while XOS with higher DP are ideal to be used as food ingredients, and MeGluA substituted XOS have shown antioxidant properties [23,60,61].

Total ion current (TIC) chromatograms obtained for the analysis of the five xylan hydrolysate samples (see Table 1) presented deceptively simple profiles. However, while some chromatographic peaks were easily identified as single compounds, many others presented multiple *m/z* signals, making the interpretation of the mass spectra challenging. Identification of X1-X6 presented in the samples was simply performed based on their retention times and mass spectra by comparison with the standards. As an example, Fig. 4(a) shows the TIC chromatogram obtained for the anal-

Table 3
Analytical performances of the HPAEC-QqQ-MS Full-scan method and LODs comparison with previous studies and with the HPAEC-QqQ-MS SRM method.

	X1	X2	X3	X4	X5	X6
Upper limit of the linear range (mg L^{-1})[a]	200	800	180	120	100	50
Regression Coefficient (R^2) (linear fit)	0.998	0.998	0.999	0.999	0.995	0.998
Repeatability intra-day (%RSD)[b]	5.27	3.05	2.27	3.42	3.03	4.31
Repeatability inter-day (%RSD)[c]	24.3	8.76	11.27	17.08	18.02	22.08
LODs (mg L^{-1}) Ref. [56]	n.a.	0.07	0.07	0.07	0.07	0.04
LODs (mg L^{-1}) Ref. [57]	0.04	0.001	0.05	0.2	0.3	0.03
LODs (mg L^{-1})[d] using full-scan method	0.311	0.003	0.003	0.008	0.049	0.059
LOQs (mg L^{-1})[d] using full-scan method	0.942	0.011	0.008	0.025	0.15	0.178
LODs (mg L^{-1})[d] using SRM method	0.104	0.001	0.001	0.001	0.013	0.021
LOQs (mg L^{-1})[d] using SRM method	0.315	0.005	0.003	0.003	0.004	0.063
S/N ratio full-scan method[e]	10.4	450.4	592.6	196.8	32.7	27
S/N ratio SRM method[e]	31.1	1069.5	5575.7	1818.9	128.7	76.7

[a] Number of data points used to define the linear range was 6.b.
[b] This parameter was obtained by injection during the same day of 10 replicates of a standard mixture containing 1 mg L^{-1} of X, 20 mg L^{-1} of X2 and 0.5 mg L^{-1} of X3-X6.
[c] This parameter was obtained by injection during three different days of 10 replicates of a standard mixture containing 1 mg L^{-1} of X1, 20 mg L^{-1} of X2 and 0.5 mg L^{-1} of X3-X6.
[d] LODs and LOQs were calculated at S/N of 3 and 10, respectively.
[e] S/N= signal-to-noise ratio. This parameter was calculated by injection of a standard mixture containing 1 mg L^{-1} of X1 and 0.5 mg L^{-1} of X2-X6.n.a= not available.

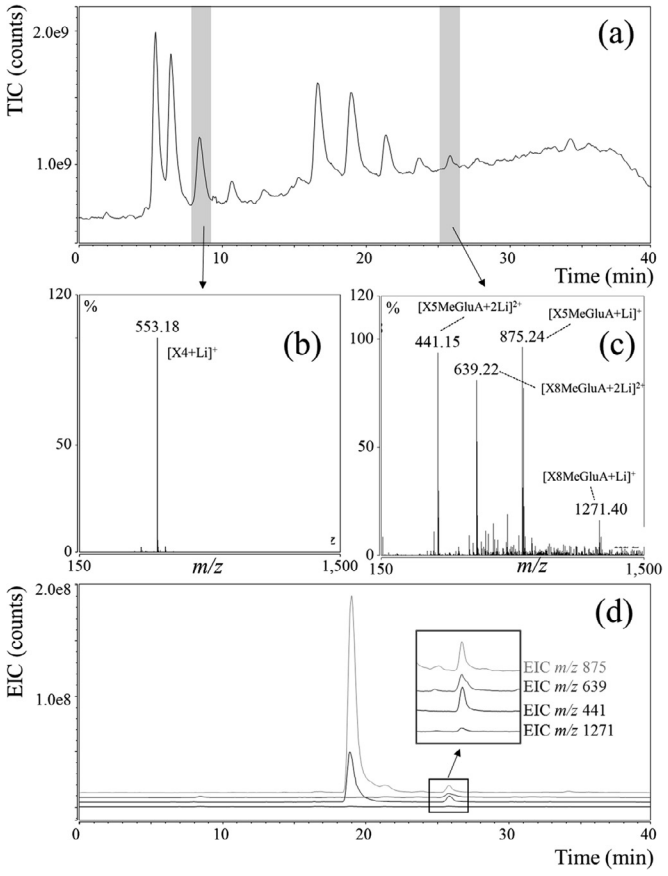

Fig. 4. Analysis of sample 4 by HPAEC-QqQ-MS: (a) Total ion current (TIC) chromatogram; (b) mass spectra for the chromatographic peaks at 7.9–8.7 min; (c) at 25.3–26.2 min; (d) overlaid extracted ion chromatograms (EICs) at *m/z* 441 $[X5MeGluA+2Li]^{2+}$, *m/z* 875 $[X5MeGluA+Li]^{+}$, *m/z* 639 $[X8MeGluA+2Li]^{2+}$ and *m/z* 1271 $[X8MeGluA+Li]^{+}$.

ysis of sample 4, Fig. 4(b) the mass spectra at retention times of 7.9–8.7 min and Fig. 4(c) the mass spectra at retention times of 25.3–26.2 min. The spectrum in Fig. 4(b) shows the simplest scenario since a single significant *m/z* was observed, and retention time and *m/z* values matched one of the available standards, i.e., X4, which eluted at 8.3 min and could be seen as the $[X4+Li]^{+}$ adduct at *m/z* 553. In contrast, Fig. 4(c) shows the complexity of the mass spectrum for other apparent 'single peaks'. In those cases, and due to the lack of standards other than X1-X6, identification was accomplished based on the *m/z* ratios detected and with aid of a list of possible beechwood enzymatic hydrolysis products assembled from literature data, which included *m/z* values for possible species generated at the ESI source. By this means, the chromatographic peak at 25.3–26.2 min (Fig. 4(c)) was identified as a mixture of X5MeGluA and X8MeGluA. Both compounds provided responses associated with singly lithium adducts, namely *m/z* 875 $[X5MeGluA+Li]^{+}$and *m/z* 1271.40 $[X8MeGluA+Li]^{+}$ and for their doubly charged lithium adducts, i.e. *m/z* 441 $[X5MeGluA+2Li]^{2+}$and *m/z* 639 $[X8MeGluA+2Li]^{2+}$. However, the EIC for *m/z* 875 $[X5MeGluA+Li]^{+}$ (Fig. 4(d)) showed a main peak at 18.9 min indicating that X5MeGluA was being eluted before 25.3–26.2 min, hence the peak at that time observed for *m/z* 875 was likely due to a fragmentation in-source of X8MeGluA, or due to the presence of an isomer of X5MeGluA being eluted at the same time than X8MeGluA. The fact that all *m/z* traces at 25.3–26.2 min presented precisely the same retention time (see Fig. 4(d) magnification), indicated that in-source fragmentation was the more probable of these options. Similar EIC traces, where a main peak was observed but also other small peaks were present, were obtained for X3MeGluA, X4MeGluA, X5MeGluA and X6MeGluA, indicating the presence of a main isomer and minor isomers/ in-source fragmentation products from bigger MeGluA XOS. Future investigations could be performed to characterise the chemical structure of each hypothetical isomer.

Using a similar approach, 19 XOS were tentatively identified within the five samples analysed in this study. In summary, a total of 25 xylooligosaccharides were detected, namely, X1, linear XOS with DP from 2 to 10 and branched XOS with one or two MeGluA groups and DP from 1 to 12. Table 4 details the 25 compounds detected in the samples analysed, including their name abbreviations, molecular formula, theoretical monoisotopic mass, experimental *m/z* values for the lithium adducts generated at the ESI source and retention times. For smaller XOS the main signal observed was for $[M+Li]^{+}$adducts, while for those XOS with molecular weight over ~800 Da, an additional signal for $[M+2Li]^{2+}$species was also significant and, for some solutes provided a higher response, or was the only species detected. Consequently, both are included in Table 4 with the species which was primarily formed highlighted in bold.

Figs. 5 and 6 compare quantitative results in g L^{-1}, when possible, i.e., for X1-X6, and their peak area *i*/peak area IS ratio (PA_i/PA_{IS}), for those compounds (*i*) which standards were un-

Table 4
HPAEC-QqQ-MS and HR-orbitrap-MS data obtained for the analysis of sample 4.

				HPAEC-QqQ-MS[a]			HR-orbitrap-MS[a]			
No.	Compound	Molecular formula	Monoisotopic mass (Da)[b]	$[M+Li]^+$ (*m/z*)	$[M+2Li]^{2+}$ (*m/z*)	Retention time (min)	$[M+Na]^+$ (*m/z*)	$[M+2Na]^{2+}$ (*m/z*)	Error (ppm)	MS^2 data (up to 3 main signals) *m/z (difference in Da from precursor)*
1	X1	$C_5H_{10}O_5$	150.0528	**157.07**	n.d.[c]	4.59	**173.0421**	n.d.[c]	0.29	155.0315 (−*18*), 113.0207 (−*60*)
2	X2	$C_{10}H_{18}O_9$	282.0951	**289.11**	n.d.[c]	5.27	**305.0844**	n.d.[c]	0.47	173.0419 (−*132*), 245.0633 (−*60*), 287.0738 (−*18*)
3	X3	$C_{15}H_{26}O_{13}$	414.1374	**421.15**	n.d.[c]	6.38	**437.1264**	n.d.[c]	−0.41	377.1056 (−*60*), 419.1162 (−*18*), 305.0846 (−*132*)
4	X4	$C_{20}H_{34}O_{17}$	546.1797	**553.18**	n.d.[c]	8.31	**569.1683**	n.d.[c]	−0.97	509.1475 (−*60*), 419.1162 (−*18–132*), 305.0846 (−*132–132*)
5	X5	$C_{25}H_{42}O_{21}$	678.222	**685.24**	n.d.[c]	10.48	**701.2107**	n.d.[c]	−0.5	641.1896 (−*60*), 551.1581 (−*18–132*), 683.2005 (−18)
6	X6	$C_{30}H_{50}O_{25}$	810.2643	**817.28**	n.d.[c]	12.73	**833.2532**	n.d.[c]	−0.21	773.2318 (−*60*), 683.2003 (−*18–132*), 815.2428 (−*18*)
7	X7	$C_{35}H_{58}O_{29}$	942.3065	949.32	**478.17**	15.11	**965.2957**	n.d.[c]	0.11	905.2760 (−*60*), 815.2426 (−*18–132*)
8	X8	$C_{40}H_{66}O_{33}$	1074.3488	1081.36	**544.19**	17.68	**1097.338**	n.d.[c]	−0.02	1037.3175 (−*60*), 947.2855 (−*18–132*), 965.2963 (−*132*)
9	X9	$C_{45}H_{74}O_{37}$	1206.3911	1213.41	**610.21**	20.32	**1229.38**	n.d.[c]	0.08	1169.3598 (−*60*), 1079.3279 (-*18–132*), 1211.3704 (−*18*)
10	X10	$C_{50}H_{82}O_{41}$	1338.4334	1345.45	**676.23**	23.18	n.d.[c]	692.2061	0.5	n.a[d]
11	X1MeGluA	$C_{12}H_{20}O_{11}$	340.1006	**347.12**	n.d.[c]	13.96	**363.0904**	n.d.[c]	0.16	n.a[d]
12	X2MeGluA	$C_{17}H_{28}O_{15}$	472.1429	**479.16**	n.d.[c]	18.3	**495.1318**	n.d.[c]	−0.53	305.0848 (−*190*)
13	X3MeGluA	$C_{22}H_{36}O_{19}$	604.1852	**611.2**	n.d.[c]	15.28	**627.1742**	n.d.[c]	−0.22	437.1266 (−*190*), 609.1637 (−*18*), 377.1056 (−*190–60*)
14	X4MeGluA	$C_{27}H_{44}O_{23}$	736.2275	**743.24**	n.d.[c]	16.51	**759.2163**	n.d.[c]	−0.35	569.1685 (−*190*), 477.1213 (−*18–132–132*), 699.1954 (−*60*)
15	X5MeGluA	$C_{32}H_{52}O_{27}$	868.2697	**875.29**	441.15	18.91	**891.2587**	n.d.[c]	−0.07	701.2107 (−*190*), 609.1638 (−*18–132–132*), 831.2380 (−*60*)
16	X6MeGluA	$C_{37}H_{60}O_{31}$	1000.312	**1007.33**	**507.17**	21.08	**1023.301**	n.d.[c]	−0.01	833.2534 (−*190*), 873.2489 (−*18–132*), 963.2810 (−*60*)
17	X7MeGluA	$C_{42}H_{68}O_{35}$	1000.312	1139.37	**573.19**	23.28	**1155.343**	n.d.[c]	−0.01	965.2961 (−*190*), 1005.2913 (−*18–132*), 1095.3233 (−*60*)
18	X8MeGluA	$C_{47}H_{76}O_{39}$	1264.3966	1271.4	**639.22**	25.35	**1287.386**	n.d.[c]	0.19	1097.3389 (−*190*), 1137.3342 (−*18–132*), 1227.3659 (−*60*)
19	X9MeGluA	$C_{52}H_{84}O_{43}$	1396.4389	1403.45	**705.24**	27.4	1419.428	**721.2085**	−0.15	626.1842 (−*95*), 691.1665 (−*30*)
20	X10MeGluA	$C_{57}H_{92}O_{47}$	1528.4811	1535.5	**771.26**	29.28	n.d.[c]	**787.2300**	0.4	n.a[d]
21	X11MeGluA	$C_{62}H_{100}O_{51}$	1660.5234	n.d.[c]	**837.28**	30.83	n.d.[c]	**853.2511**	0.41	758.2266 (−*95*), 823.2095 (−*30*)
22	X12MeGluA	$C_{67}H_{108}O_{55}$	1792.5657	n.d.[c]	**903.3**	32.73	n.d.[c]	**919.2733**	0.11	824.2471 (−*95*)
23	X7MeGluA2	$C_{49}H_{78}O_{41}$	1322.4021	1329.42	**668.22**	33.79	n.d.[c]	**684.1899**	−0.43	589.1663 (−*95*), 654.1793 (−*30*)
24	X8MeGluA2	$C_{54}H_{86}O_{45}$	1454.4444	n.d.[c]	**734.24**	35.19	n.d.[c]	**750.211**	−0.35	655.1872 (−*95*), 720.2018 (−*30*), 560.1626 (−*190*)
25	X9MeGluA2	$C_{59}H_{94}O_{49}$	1586.4866	n.d.[c]	**800.26**	36.68	n.d.[c]	**816.2323**	−0.14	n.a[d]

[a] Marked in bold: specie which provided higher response.
[b] Exact mass calculated using the mass of the most abundant isotope of each element.
[c] Not detected.
[d] Not available due to the precursor ion signal being too small.

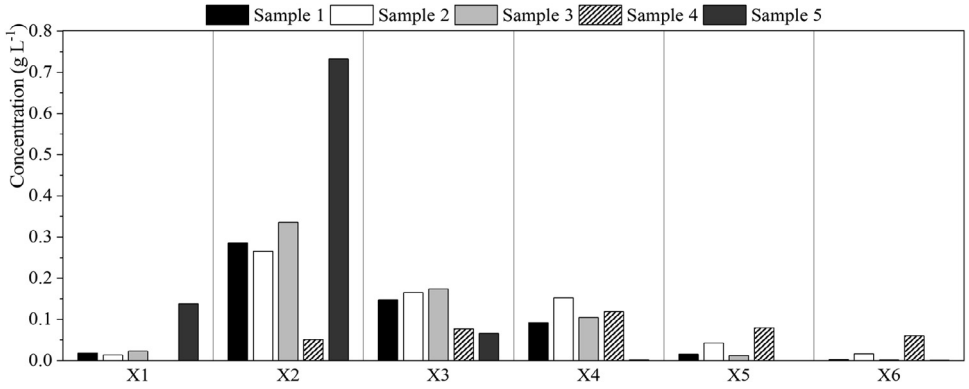

Fig. 5. Quantitation results for linear X1-X6 in samples 1–5 (Table 1) using the HPAEC-QqQ-MS developed in this study (instrumental parameters detailed in Table 2).

available, amongst samples 1–5. While it was previously observed that smaller peak areas did not necessarily correspond with lower concentration, relative PA_i/PA_{IS} ratio can be used to quantitatively compare the amount of a specific compound obtained according to the different enzymatic hydrolysis conditions applied.

Although, the number of samples analysed was limited and an exhaustive evaluation of the relationship between hydrolysis conditions and XOS generated is out of the scope of this study, the results obtained clearly showed the potential of the HPAEC-QqQ-MS method to help tailor future XOS production. For example, XOS with DP > 9 were only produced at temperatures < 50 °C and pH 4.0. Likewise, if comparing samples 4 and 5, produced by using the continuous flow microfluidic reactor and 25 °C, a change in pH from 4.0 to 5.0 significantly affected the XOS profile produced. At pH 4.0, X2-X6 were obtained while at pH 5.0 only X1-X3 were produced, and at significantly higher concentration. Regarding acidic XOS produced under those conditions, at pH 4.0 the whole range of X1MeGluA to X12MeGluA was present, whilst at pH 5.0, X3MeGluA, X4MeGluA and X5MeGluA were favourably produced. Combining these results, it is clear that by using low pH and low temperature during hydrolysis the production of a wider range of XOS was promoted. Fig. 7 shows EICs for the 25 compounds identified from the analysis of sample 4, which was the only sample which contained all species. It is important to highlight that some of these compounds were partially or completely coeluted and could thus be wrongly assigned as single compounds when using HPAEC with PAD, clearly emphasising the significance of the benefits of exploiting MS detection for the analysis of XOS in such complex samples.

3.4. Confirmation of compound identities by HR-Orbitrap-MS

The identities of the 19 compounds provisionally identified by HPAEC-QqQ-MS were further confirmed using accurate-mass high-resolution ESI-HR-Orbitrap-MS. To perform these experiments, samples were diluted ten times using DIW:0.5 mM LiCl/MeOH (9:1) and directly infused into the ESI source of the HR-Orbitrap-MS using a syringe pump at a flow rate of 10 µL min^{-1}. As samples were injected directly, without any previous separation, and as they contained approx. 5 mM sodium citrate buffer used for the

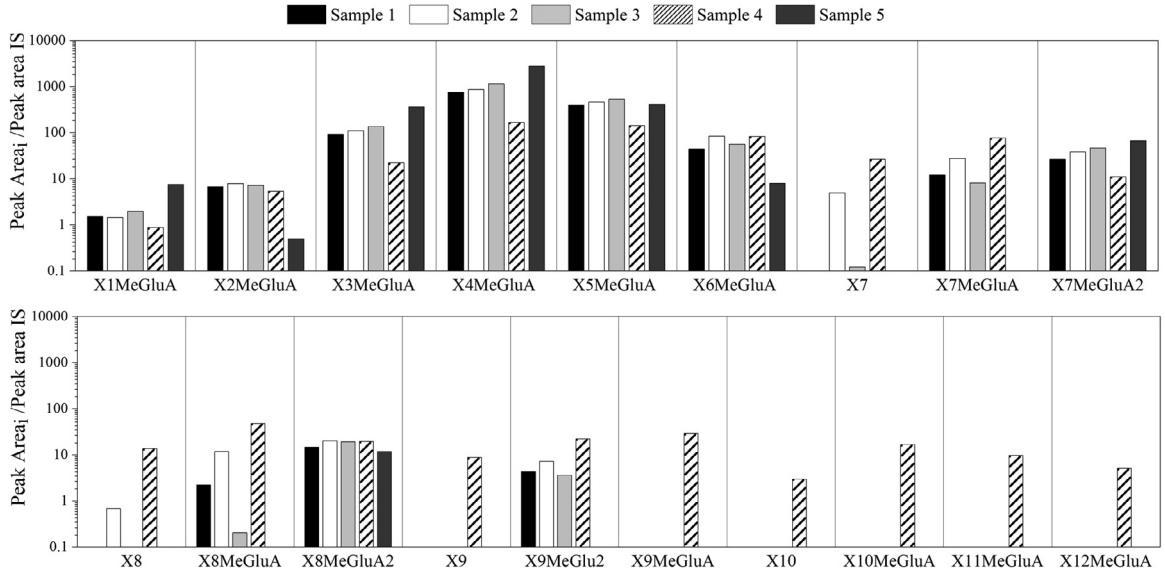

Fig. 6. Peak area$_i$/Peak area$_{IS}$ ratio results for linear X7-X10 and MeGluA XOS derivatives detected in samples 1–5 (Table 1) using the HPAEC-QqQ-MS developed in this study (instrumental parameters detailed in Table 2). *i*= individual XOS; IS=internal standard.

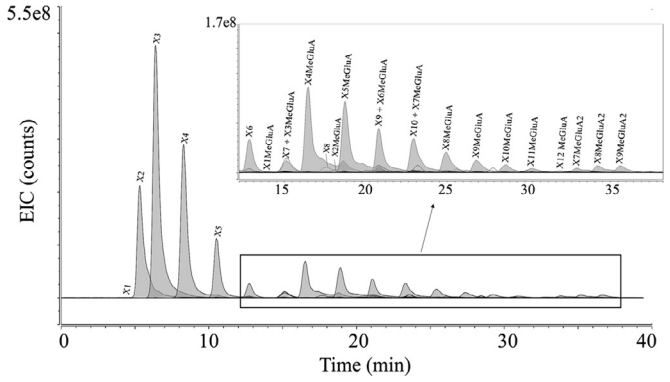

Fig. 7. Overlaid extracted ion chromatograms (EICs) of $[M+Li]^+$ adducts (see Table 4 for *m/z* extracted) for the 25 compounds identified in the analysis of sample 4 (see Table 1) using the HPAEC-QqQ-MS developed in this study (instrumental parameters detailed in Table 2).

enzymatic hydrolysis treatment, $[M+Na]^+$ adducts of the XOS were favourably formed instead of $[M+Li]^+$ species. When the samples were analysed using HPAEC-QqQ-MS, sodium was unretained and being eluted at the beginning of the analysis and, hence, did not interfere with the formation of XOS $[M+Li]^+$ adducts at the ESI source. To confirm the species identity, accurate-mass for precursor ions and MS^2 data was used, including accurate-mass for the fragments and for the neutral losses produced during fragmentation. Accurate determination of the monoisotopic mass, providing up to four accurate decimal figures, restricted the pool of possible elemental composition combinations significantly, even more so considering targeted compounds in this study were compounds containing C, H and O only. As an example, Table 4 details the results obtained for the analysis of sample 4, which contained all the compounds tentatively identified by QqQ-MS. Table 4 includes *m/z* values providing higher responses for targeted compounds, molecular formula provided for each *m/z*, error and MS^2 data when the experiments were successful. Occasionally, the signal for the precursor ion was too weak to carry out MS^2 experiments, hence confirmation of the identity was only based on the formula provided through the accurate mass.

Fig. 8 shows the Full MS(+) spectrum obtained for sample 4. The predominant ions observed in the mass spectrum of sample 4 corresponded to sodium adducts, singly charged $[M+Na]^+$ or doubly charged $[M+2Na]^{2+}$. The molecular formulas provided by the orbitrap for those predominant ions confirmed the identity of all compounds tentatively identified by HPAEC-QqQ-MS with mass accuracy lower than 1 ppm (see Table 4). To further confirm the identities proposed for the targeted ions in the full MS(+) spectrum, MS^2 was performed on each of those ions. Data about neutral losses observed and main fragments produced are detailed in Table 4. As an example, the MS^2 spectrum obtained for $[X8+Na]^+$ (*m/z* 1097.3378) is presented at Fig. 9 where the fragment ions formed were named according to the nomenclature proposed by Domon and Costello [62]. Briefly, according to this nomenclature, A_i, B_i and C_i labels are used to designate fragments containing a non-reducing end sugar unit, whereas X_i, Y_i and Z_i correspond to ions still containing the reducing sugar unit. Subscripts indicate the position relative to the termini and superscripts indicate cleavages within the carbohydrate rings. The MS^2 X8 spectrum showed the typical fragments expected for neutral linear oligosaccharides [27], namely, fragments resulting from three fragmentation pathways: (a) glycosidic cleavages (C-type fragments) with consecutive losses of xylosyl residues (132 Da) from the precursor ion at *m/z* 965.2963 (C_7), *m/z* 833.2538 (C_6), *m/z* 701.2114 (C_5) and *m/z* 569.1687 (C_4); (b) cross-ring cleavages (A-type fragments) occurring with losses of 60 and 90 Da at *m/z* 1037.3175 ($^{0,2}A_8$) and *m/z* 1007.3074 ($^{0,3}A_8$), respectively, and (c) from losing water with the formation of ion at *m/z* 1079.3284 (B_8) from the precursor ion, followed by successive losses of xylosyl residues (132 Da) yielding the fragment ions at *m/z* 947.2855 (B_7), *m/z* 815.2431 (B_6) and *m/z* 683.2007 (B_5). The C-type fragments observed could have also corresponded to Y-type fragments but herein they have been assigned as C-type according to Reis et al. [39] who reported that (1→4)-linked glucose residues exhibit C-type fragments. Fig. 1S and Fig. 2S at Supplementary data show additional examples of MS^2 spectra obtained for singly charged sodium adducts of X4 substituted with one 4-*O*-methylglucoronic acid (X4MeGluA) at *m/z* 759.2163 and double charged sodium adducts of X8 substituted with two MeGluA (X8MeGluA2) at *m/z* 750.2110, respectively. These spectra showed a major fragment ion formed by the loss of 190 Da from $[X4MeGluA+Na]^+$ at *m/z* 569.1685 or by the loss of 95 Da from $[X8MeGluA2+2Na]^{2+}$at *m/z* 655.1872. This fragmentation pathway involved cleavage of the glycosidic linkage between the xylose linear chain and the substitution residue, with loss of the acidic

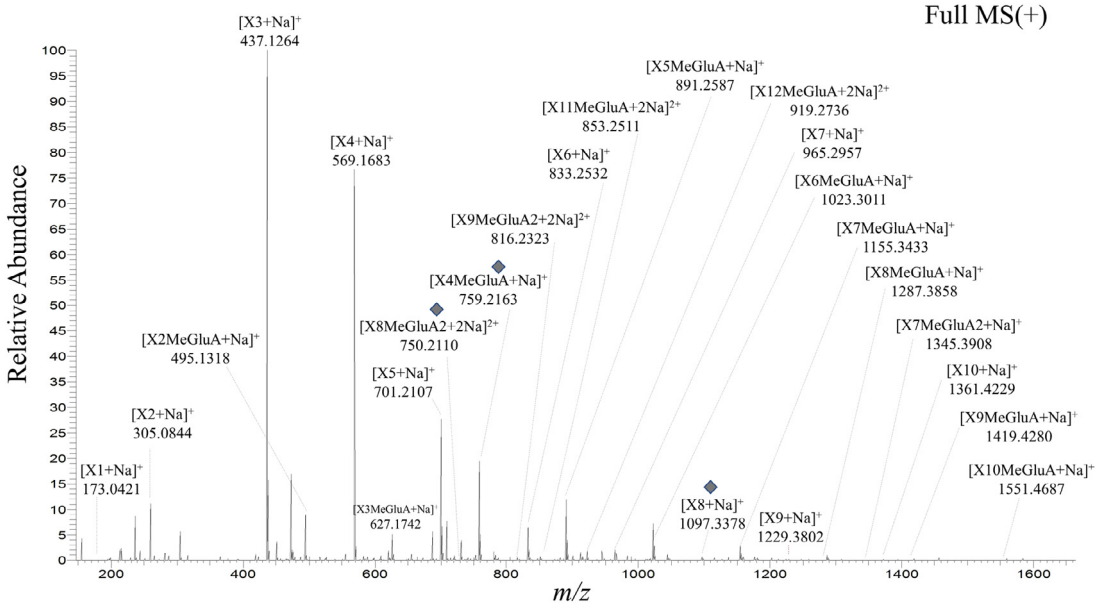

Fig. 8. Full MS(+) spectrum provided by HR-orbitrap-MS of the xylooligosaccharides (XOS) products in sample 4 (see Table 1).

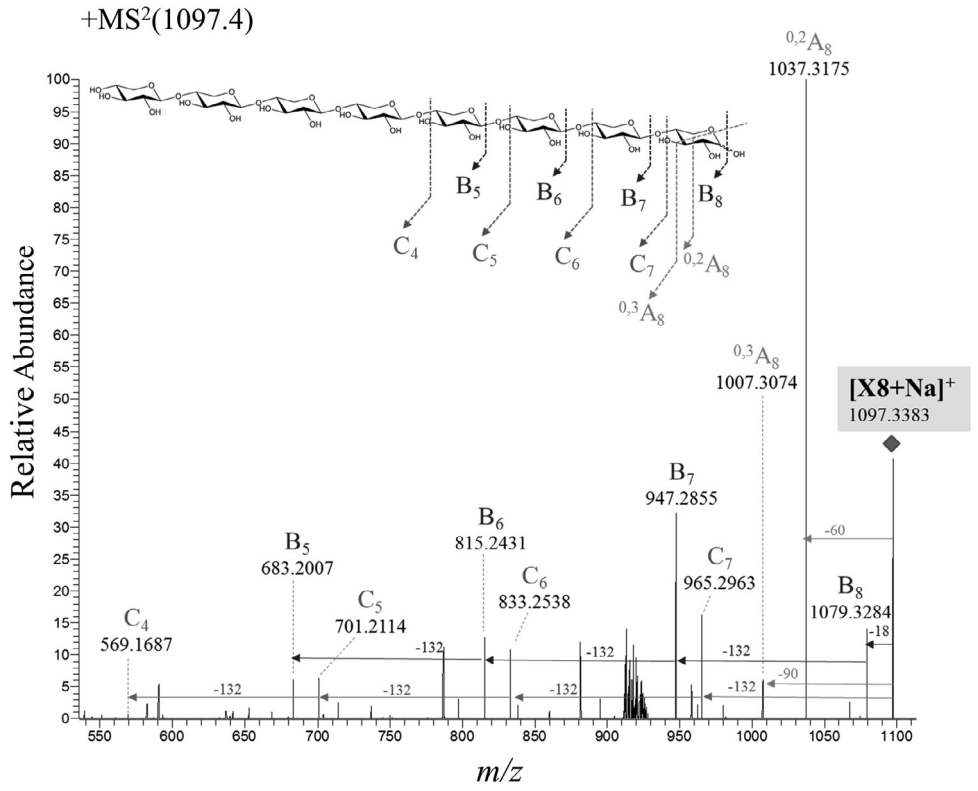

Fig. 9. +MS^2 spectra of the singly sodiated X8. Schematic fragmentation pathway is illustrated and ions were labelled according to the nomenclature proposed by Domon and Costello [62].

decoration (MeGluA). The presence of a second MeGluA group in X8MeGluA2 was confirmed by the formation of a second fragment ion at *m/z* 560.1626 generated by the loss of 190 Da from the double charged precursor ion. The MS^2 spectrum of X8MeGluA2 did not show significant additional fragments, likely due to the low abundance of the precursor ion. However, the X4MeGluA precursor ion was more abundant and produced some other important fragment ions. Since these samples were injected directly, without any previous separation, four structural isomers of X4MeGluA, i.e. with the MeGluA moiety besides the xylose unit at the non-reducing end (isomer 1), besides the xyloses at two middle positions (isomers 2 and 3) or besides the xylose at the reducing end (isomer 4), could be present. Additional information regarding the assignment of those fragments can be found within the Supplementary Information. In summary, these spectra have supported the proposition of a MeGluA residue at the reducing end (isomer 4) and/or at the non-reducing end (isomer 1) of the X4MeGluA. However, the presence of all four isomers cannot be excluded. Nevertheless, the

main objective of the analysis carried out by HR-Orbitrap-MS was the confirmation of the identity of the main compounds detected by HPAEC-QqQ-MS and the data provided by these analyses, i.e., molecular formulas and main MS^2 fragmentation pathways (see Table 4), confirmed the identity of the 19 compounds tentatively identified by HPAEC-QqQ-MS.

3.5. Selected reaction monitoring (SRM) acquisition mode

Aiming to demonstrate the capability of HPAEC-QqQ-MS to determine targeted XOS present in low concentrations, a new method was developed using selected reaction monitoring (SRM) for the XOS standards available (X1-X6). SRM acquisition mode is the key operating mode for target compound quantitation with a triple quadrupole MS. The SRM transitions were automatically optimised using a software tool which provided, from a selected ion precursor, the optimal fragment ions, optimal collision energy and optimal RF Lens voltage. For this purpose, a mixture of X1-X6 at concentration of 10 mg L^{-1} was directly infused into the HPAEC and make-up stream just before the ESI source employing a T-connection and a syringe pumping the sample at 10 µL min^{-1}. Eluent composition was set at 50% B to mimic average mobile phase concentration during a 'real' analysis. In addition to the optimal or primary SRM transitions obtained during the automatic optimisation, a SRM method containing SRM transitions monitoring *m/z* $[M+Li]^+ \rightarrow [M+Li]^+$, sometimes referred as 'not real' SRM transitions, were added as secondary SRM transitions for each targeted XOS. Both primary and secondary SRM transitions were assessed experimentally by analysing a mixture of X1-X6 containing 1 mg L^{-1} of X1 and 0.5 mg L^{-1} of X2-X6 using the developed SRM method and the response of each SRM transition for each solute was compared. Those SRM transitions which provided better response were chosen as optimal. Table 2 summarises the SRM transitions used in the SRM method for the target solutes. LODs and S/N ratios were also calculated for the SRM method and these results are shown in Table 3. As expected, the SRM method provided higher S/N ratio than full-scan acquisition mode for all standards tested, hence providing lower LODs. SRM offers a solution to analyse very dilute samples, thus eliminating possible undesirable matrix effects or simply allowing the detection of targeted solutes present in the samples at very low concentration levels. While SRM is highly selective and sensitive, this approach has disadvantages which are characteristic to the targeted acquisition, as only solutes included in the SRM acquisition method will be detected. Future studies focused on the characterisation of XOS in different LCB material could assist in the creation of a more comprehensive SRM method, which could include SRM transitions for all targeted compounds present in different LCB materials.

4. Conclusions

A new method for the determination of XOS produced by hydrolysis of xylan have been developed. A simple sample treatment of the hydrolysates was required, namely, 10-fold dilution and filtration. XOS present on the diluted hydrolysates were separated by HPAEC using a high-resolution CarboPac PA200 column and binary gradient program based on 150 mM NaOH and 150 mM NaOAc eluents. For the first time, HPAEC was directly coupled with ESI-QqQ-MS allowing the separation and identification of the XOS present in the samples in one workflow without the need of additional steps, such as fractionation and desalting steps for MS detection and/or using additional techniques for XOS characterisation such as NMR. Evaluation of separation, eluent suppression, ionisation and detection conditions were carried out using available standards, i.e., X1-X6 and delivered the lowest LODs reported in the literature for an IC-MS based method. The method developed was applied for the determination of the XOS present in five samples produced by using different enzymatic hydrolysis conditions. In summary, a total of 25 XOS were detected, namely, X1, linear XOS with DP from 2 to 10 and branched XOS with one or two MeGluA groups and DP from 1 to 12, showing the ability of the new method for the identification of linear and branched XOS in complex mixtures. Identity of the compounds detected by HPAEC-QqQ-MS was further validated using HR-orbitrap-MS. The XOS profile was different for each sample analysed since hydrolysates composition is a function of the conditions applied for the hydrolysis. Therefore, this study demonstrated the applicability of the method developed as a new simple and fast analytical tool to tailor XOS production to suit desired applications based upon their DP, and type and number of substituents.

Declaration of Competing Interest

The authors declare that they have no known competing financial interests or personal relationships that could have appeared to influence the work reported in this paper.

CRediT authorship contribution statement

Estrella Sanz Rodríguez: Conceptualization, Methodology, Formal analysis, Investigation, Validation, Writing – original draft. **Gloria Lizeth Díaz-Arenas:** Conceptualization, Investigation, Writing – review & editing. **Stefan Makart:** Conceptualization, Writing – review & editing. **Debjani Ghosh:** Conceptualization, Investigation, Writing – review & editing. **Antonio Frank Patti:** Conceptualization, Supervision, Writing – review & editing. **Gil Garnier:** Conceptualization, Supervision, Writing – review & editing, Resources, Funding acquisition. **Joanne Tanner:** Conceptualization, Supervision, Writing – review & editing, Resources, Funding acquisition. **Brett Paull:** Conceptualization, Supervision, Writing – review & editing, Resources, Funding acquisition.

Acknowledgments

Authors would like to thank the University of Tasmania and the ARC Industrial Transformation Research Hub for Processing Advanced Lignocellulosics (PALS) for their financial support (Grant: ARC IH170100020). The authors acknowledge Thermo Fisher Scientific for placement of the IC-QqQ-MS instrument within the University of Tasmania to undertake this work. We would also like to acknowledge the help of Dr. Noel Davies and Dr. David Nicholson of the Central Science Laboratory (CSL), University of Tasmania, for provision of technical support for the HR-orbitrap-MS analysis.

Supplementary materials

Supplementary material associated with this article can be found, in the online version, at doi:10.1016/j.chroma.2022.462836.

References

[1] A.F.A. Carvalho, P.D.O. Neto, D.F. da Silva, G.M. Pastore, Xylo-oligosaccharides from lignocellulosic materials: chemical structure, health benefits and production by chemical and enzymatic hydrolysis, Food Res. Int. 51 (1) (2013) 75–85, doi:10.1016/j.foodres.2012.11.021.
[2] L. Santibáñez, C. Henríquez, R. Corro-Tejeda, S. Bernal, B. Armijo, O. Salazar, Xylooligosaccharides from lignocellulosic biomass: a comprehensive review, Carbohydr. Polym. (2021) 251, doi:10.1016/j.carbpol.2020.117118.
[3] A.A. Aachary, S.G. Prapulla, Xylooligosaccharides (XOS) as an emerging prebiotic: microbial synthesis, utilization, structural characterization, bioactive properties, and applications, Compr. Rev. Food Sci. Food Saf. 10 (1) (2011) 2–16, doi:10.1111/j.1541-4337.2010.00135.x.
[4] G.I.R. Report, Global Xylooligosaccharides (XOS) Market 2021 by Manufacturers, Regions, Type and Application, Forecast to 2026. https://www.globalinforesearch.com/reports/520714/xylooligosaccharides-xos, 2021 (accessed 25 November 2021).

[5] A.K. Samanta, N. Jayapal, C. Jayaram, S. Roy, A.P. Kolte, S. Senani, M. Sridhar, Xylooligosaccharides as prebiotics from agricultural by-products: production and applications, Bioact. Carbohydr. Diet. Fibre 5 (1) (2015) 62–71, doi:10.1016/j.bcdf.2014.12.003.
[6] C. Amorim, S.C. Silvério, K.L.J. Prather, L.R. Rodrigues, From lignocellulosic residues to market: production and commercial potential of xylooligosaccharides, Biotechnol. Adv. 37 (7) (2019), doi:10.1016/j.biotechadv.2019.05.003.
[7] P. Poletto, G.N. Pereira, C.R.M. Monteiro, M.A.F. Pereira, S.E. Bordignon, D. de Oliveira, Xylooligosaccharides: transforming the lignocellulosic biomasses into valuable 5-carbon sugar prebiotics, Process Biochem. 91 (2020) 352–363, doi:10.1016/j.procbio.2020.01.005.
[8] V. Kumar, A. Bahuguna, S. Ramalingam, M. Kim, Developing a sustainable bioprocess for the cleaner production of xylooligosaccharides: an approach towards lignocellulosic waste management, J. Clean. Prod. (2021) 316, doi:10.1016/j.jclepro.2021.128332.
[9] Q. Qing, H. Li, R. Kumar, C.E. Wyman, Xylooligosaccharides production, quantitation, and characterization in context of lignocellulosic biomass pretreatment, in: Aqueous Pretreatment of Plant Biomass for Biological and Chemical Conversion to Fuels and Chemicals, Wiley Series in Renewable Resources, 2013, pp. 391–415, doi:10.1002/9780470975831.ch19.
[10] A. Palaniappan, V.G. Balasubramaniam, U. Antony, Prebiotic potential of xylooligosaccharides derived from finger millet seed coat, Food Biotechnol. 31 (4) (2017) 264–280, doi:10.1080/08905436.2017.1369433.
[11] A. Cano, C. Palet, Xylooligosaccharide recovery from agricultural biomass waste treatment with enzymatic polymeric membranes and characterization of products with MALDI-TOF-MS, J. Membr. Sci. 291 (1–2) (2007) 96–105, doi:10.1016/j.memsci.2006.12.048.
[12] R. Bhatia, A. Winters, D.N. Bryant, M. Bosch, J. Clifton-Brown, D. Leak, J. Gallagher, Pilot-scale production of xylo-oligosaccharides and fermentable sugars from Miscanthus using steam explosion pretreatment, Bioresour. Technol. (2020) 296, doi:10.1016/j.biortech.2019.122285.
[13] L.B. Brenelli, F.L. Figueiredo, A. Damasio, T.T. Franco, S.C. Rabelo, An integrated approach to obtain xylo-oligosaccharides from sugarcane straw: from lab to pilot scale, Bioresour. Technol. (2020) 313, doi:10.1016/j.biortech.2020.123637.
[14] M. Chemin, A.L. Wirotius, F. Ham-Pichavant, G. Chollet, D. Da Silva Perez, M. Petit-Conil, H. Cramail, S. Grelier, Well-defined oligosaccharides by mild acidic hydrolysis of hemicelluloses, Eur. Polym. J. 66 (2015) 190–197, doi:10.1016/j.eurpolymj.2015.02.008.
[15] C. de Oliveira Gorgulho Silva, J.A. de Aquino Ribeiro, A.L. Souto, P.V. Abdelnur, L.R. Batista, K.A. Rodrigues, N.S. Parachin, E.X.F. Filho, Sugarcane bagasse hydrothermal pretreatment liquors as suitable carbon sources for hemicellulase production by aspergillus niger, BioEnergy Res. 11 (2) (2018) 316–329, doi:10.1007/s12155-018-9898-z.
[16] V. Guigon, C. Chirat, L. Fort, D. Lachenal, Characterization of enzyme-resistant xylooligosaccharides extracted from hardwood chips by pre-hydrolysis and further depolymerized by enzymatic treatment, Holzforschung 74 (2) (2020) 123–130, doi:10.1515/hf-2018-0249.
[17] J.A. Linares-Pastén, A. Aronsson, E. Nordberg Karlsson, Structural considerations on the use of endo-xylanases for the production of prebiotic xylooligosaccharides from biomass, Curr. Protein Pept. Sci. 19 (1) (2018) 48–67, doi:10.2174/1389203717666160923155209.
[18] E. Nordberg Karlsson, E. Schmitz, J.A. Linares-Pastén, P. Adlercreutz, Endo-xylanases as tools for production of substituted xylooligosaccharides with prebiotic properties, Appl. Microbiol. Biotechnol. 102 (21) (2018) 9081–9088, doi:10.1007/s00253-018-9343-4.
[19] W. Zhang, B. Zhang, L. Zhang, J. Jiang, Progress on Production of xylo-oligosaccharides from lignocellulosic materials by non-enzymatic catalysis, Chem. Ind. For. Prod. 40 (6) (2020) 118–128, doi:10.3969/j.issn.0253-2417.2020.06.015.
[20] N. Arumugam, P. Biely, V. Puchart, A.S. Gerrano, K. De Mukherjee, S. Singh, S. Pillai, Xylan from bambara and cowpea biomass and their structural elucidation, Int. J. Biol. Macromol. 132 (2019) 987–993, doi:10.1016/j.ijbiomac.2019.04.030.
[21] S.L. Chong, T. Nissilä, R.A. Ketola, S. Koutaniemi, M. Derba-Maceluch, E.J. Mellerowicz, M. Tenkanen, P. Tuomainen, Feasibility of using atmospheric pressure matrix-assisted laser desorption/ionization with ion trap mass spectrometry in the analysis of acetylated xylooligosaccharides derived from hardwoods and Arabidopsis thaliana, Anal. Bioanal. Chem. 401 (9) (2011) 2995–3009, doi:10.1007/s00216-011-5370-z.
[22] C. Brasseur, J. Bauwens, C. Tarayre, C. Mattéotti, P. Thonart, J. Destain, F. Francis, E. Haubruge, D. Portetelle, M. Vandenbol, J.F. Focant, E. De Pauw, MALDI-TOF ms analysis of cellodextrins and xylo-oligosaccharides produced by hindgut homogenates of reticulitermes santonensis, Molecules 19 (4) (2014) 4578–4594, doi:10.3390/molecules19044578.
[23] M.A. Kabel, H.A. Schols, A.G.J. Voragen, Mass determination of oligosaccharides by matrix-assisted laser desorption/ionization time-of-flight mass spectrometry following HPLC, assisted by on-line desalting and automated sample handling, Carbohydr. Polym. 44 (2) (2001) 161–165, doi:10.1016/S0144-8617(00)00203-4.
[24] Y. Nakahara, K. Yamauchi, S. Saka, MALDI-TOF/MS analyses of decomposition behavior of beech xylan as treated by semi-flow hot-compressed water, J. Wood Sci. 60 (3) (2014) 225–231, doi:10.1007/s10086-014-1396-0.
[25] V. Puchart, L. Fraňová, K.B.R. Mørkeberg Krogh, T. Hoff, P. Biely, Action of different types of endoxylanases on eucalyptus xylan *in situ*, Appl. Microbiol. Biotechnol. 102 (4) (2018) 1725–1736, doi:10.1007/s00253-017-8722-6.
[26] B. Quéméner, J.J. Ordaz-Ortiz, L. Saulnier, Structural characterization of underivatized arabino-xylo-oligosaccharides by negative-ion electrospray mass spectrometry, Carbohydr. Res. 341 (11) (2006) 1834–1847, doi:10.1016/j.carres.2006.04.039.
[27] A. Reis, M.A. Coimbra, P. Domingues, A.J. Ferrer-Correia, M. Rosário, M. Domingues, Structural characterisation of underivatised olive pulp xylo-oligosaccharides by mass spectrometry using matrix-assisted laser desorption/ionisation and electrospray ionisation, Rapid Commun. Mass Spectrom. 16 (22) (2002) 2124–2132, doi:10.1002/rcm.839.
[28] L. Wei, L. Liu, Z. Bian, Y. Wu, MALDI-TOF-MS analysis of hydrolysis products of beechwood and birchwood xylans catalyzed by xylanase from Bacillus subtilis, J. Food Biochem. 45 (8) (2021), doi:10.1111/jfbc.13841.
[29] A. Jacobs, P.T. Larsson, O. Dahlman, Distribution of uronic acids in xylans from various species of soft- and hardwood as determined by MALDI Mass spectrometry, Biomacromolecules 2 (3) (2001) 979–990, doi:10.1021/bm010062x.
[30] L. Testova, S.L. Chong, M. Tenkanen, H. Sixta, Autohydrolysis of birch wood, Holzforschung 65 (4) (2011) 535–542, doi:10.1515/HF.2011.073.
[31] Y. Deng, C. Chen, L. Chen, B. Han, S. Li, J. Zhao, Fast saccharide mapping method for quality consistency evaluation of commercial xylooligosaccharides collected in China, J. Pharm. Anal. 11 (3) (2021) 284–291, doi:10.1016/j.jpha.2020.08.013.
[32] M.J. Bowman, B.S. Dien, R.E. Hector, G. Sarath, M.A. Cotta, Liquid chromatography-mass spectrometry investigation of enzyme-resistant xylooligosaccharide structures of switchgrass associated with ammonia pretreatment, enzymatic saccharification, and fermentation, Bioresour. Technol. 110 (2012) 437–447, doi:10.1016/j.biortech.2012.01.062.
[33] M. Juvonen, M. Kotiranta, J. Jokela, P. Tuomainen, M. Tenkanen, Identification and structural analysis of cereal arabinoxylan-derived oligosaccharides by negative ionization HILIC-MS/MS, Food Chem. 275 (2019) 176–185, doi:10.1016/j.foodchem.2018.09.074.
[34] M.A. Kabel, P. De Waard, H.A. Schols, A.G.J. Voragen, Location of O-acetyl substituents in xylo-oligosaccharides obtained from hydrothermally treated eucalyptus wood, Carbohydr. Res. 338 (1) (2003) 69–77, doi:10.1016/S0008-6215(02)00351-8.
[35] M.A. Kabel, H.A. Schols, A.G.J. Voragen, Complex xylo-oligosaccharides identified from hydrothermally treated eucalyptus wood and brewery's spent grain, Carbohydr. Polym. 50 (2) (2002) 191–200, doi:10.1016/S0144-8617(02)00022-X.
[36] S. Pasanen, J. Jänis, P. Vainiotalo, Cello-, malto- and xylooligosaccharide fragmentation by collision-induced dissociation using QIT and FT-ICR mass spectrometry: a systematic study, Int. J. Mass Spectrom. 263 (1) (2007) 22–29, doi:10.1016/j.ijms.2006.12.002.
[37] J. Pu, X. Zhao, L. Xiao, H. Zhao, Development and validation of a HILIC-ELSD method for simultaneous analysis of non-substituted and acetylated xylo-oligosaccharides, J. Pharm. Biomed. Anal. 139 (2017) 232–237, doi:10.1016/j.jpba.2017.03.007.
[38] A. Reis, M.A. Coimbra, P. Domingues, A.J. Ferrer-Correia, M.R.M. Domingues, Fragmentation pattern of underivatised xylo-oligosaccharides and their alditol derivatives by electrospray tandem mass spectrometry, Carbohydr. Polym. 55 (4) (2004) 401–409, doi:10.1016/j.carbpol.2003.11.001.
[39] A. Reis, M.R.M. Domingues, A.J. Ferrer-Correia, M.A. Coimbra, Structural characterisation by MALDI-MS of olive xylo-oligosaccharides obtained by partial acid hydrolysis, Carbohydr. Polym. 53 (1) (2003) 101–107, doi:10.1016/S0144-8617(03)00007-9.
[40] A. Reis, P. Pinto, D.V. Evtuguin, C.P. Neto, P. Domingues, A.J. Ferrer-Correia, M.R.M. Domingues, Electrospray tandem mass spectrometry of underivatised acetylated xylo-oligosaccharides, Rapid Commun. Mass Spectrom. 19 (23) (2005) 3589–3599, doi:10.1002/rcm.2234.
[41] T. Fouquet, H. Sato, Y. Nakamichi, A. Matsushika, H. Inoue, Electrospray multistage mass spectrometry in the negative ion mode for the unambiguous molecular and structural characterization of acidic hydrolysates from 4-O-methylglucuronoxylan generated by endoxylanases, J. Mass Spectrom. 54 (3) (2019) 213–221, doi:10.1002/jms.4321.
[42] B. Quéméner, J. Vigouroux, E. Rathahao, J.C. Tabet, A. Dimitrijevic, M. Lahaye, Negative electrospray ionization mass spectrometry: a method for sequencing and determining linkage position in oligosaccharides from branched hemicelluloses, J. Mass Spectrom. 50 (1) (2015) 247–264, doi:10.1002/jms.3528.
[43] X. Xiao, J.Y. Wen, Y.Y. Wang, J. Bian, M.F. Li, F. Peng, R.C. Sun, NMR and ESI–MS spectrometry characterization of autohydrolysis xylo-oligosaccharides separated by gel permeation chromatography, Carbohydr. Polym. 195 (2018) 303–310, doi:10.1016/j.carbpol.2018.04.088.
[44] M.A. Kabel, H.A. Schols, A.G.J. Voragen, Identification of structural features of various (O-acetylated) xylo-oligosaccharides from xylan-rich agricultural by-products: a review, ACS Symp. Ser. (2004) 108–121.
[45] R.D. Rocklin, C.A. Pohl, Determination Of Carbohydrates by anion exchange chromatography with pulsed amperometric detection, J. Liq. Chromatogr. 6 (9) (1983) 1577–1590, doi:10.1080/01483918308064876.
[46] M.H. Chen, K. Rajan, D.J. Carrier, V. Singh, Separation of xylose oligomers from autohydrolyzed Miscanthus × giganteus using centrifugal partition chromatography, Food Bioprod. Process. 95 (2015) 125–132, doi:10.1016/j.fbp.2015.04.006.
[47] H. Li, Q. Qing, R. Kumar, C.E. Wyman, Chromatographic determination of 1, 4-β-xylooligosaccharides of different chain lengths to follow xylan deconstruction in biomass conversion, J. Ind. Microbiol. Biotechnol. 40 (6) (2013) 551–559, doi:10.1007/s10295-013-1254-x.

[48] B. Yang, C.E. Wyman, Characterization of the degree of polymerization of xylooligomers produced by flowthrough hydrolysis of pure xylan and corn stover with water, Bioresour. Technol. 99 (13) (2008) 5756–5762, doi:10.1016/j.biortech.2007.10.054.
[49] N. Rumachik, T. Tian, Y. Hou, C. Saini, J. Cheng, C. Pohl, Y. Liu, Towards a more complete glycome: advances in ion chromatography-mass spectrometry (IC-MS) for improved separation and analysis of carbohydrates, J. Chromatogr. B Anal. Technol. Biomed. Life Sci. (2021) 1175, doi:10.1016/j.jchromb.2021.122719.
[50] E. Sanz Rodriguez, M.M.G. Perron, M. Strzelec, B.C. Proemse, A.R. Bowie, B. Paull, Analysis of levoglucosan and its isomers in atmospheric samples by ion chromatography with electrospray lithium cationisation - Triple quadrupole tandem mass spectrometry, J. Chromatogr. A 1610 (2020), doi:10.1016/j.chroma.2019.460557.
[51] R. Tedesco, E. Barbaro, R. Zangrando, A. Rizzoli, V. Malagnini, A. Gambaro, P. Fontana, G. Capodaglio, Carbohydrate determination in honey samples by ion chromatography–mass spectrometry (HPAEC-MS), Anal. Bioanal. Chem. 412 (22) (2020) 5217–5227, doi:10.1007/s00216-020-02732-3.
[52] D. Ghosh, A.B. Vir, G. Garnier, A.F. Patti, J. Tanner, Continuous flow production of xylooligosaccharides by enzymatic hydrolysis, Chem. Eng. Sci. (2021) 244, doi:10.1016/j.ces.2021.116789.
[53] Thermo Fisher Scientific. CarboPac PA200-Product Manual. 031992 Revision02. November 2018. https://tools.thermofisher.com/content/sfs/manuals/38510-31992-01_CP_PA200_V21.pdf (accessed 15 Sep 2020).
[54] A. Reis, M.R.M. Domingues, P. Domingues, A.J. Ferrer-Correia, M.A. Coimbra, Positive and negative electrospray ionisation tandem mass spectrometry as a tool for structural characterisation of acid released oligosaccharides from olive pulp glucuronoxylans, Carbohydr. Res. 338 (14) (2003) 1497–1505, doi:10.1016/S0008-6215(03)00196-4.
[55] M.J. Kailemia, L.R. Ruhaak, C.B. Lebrilla, I.J. Amster, Oligosaccharide analysis by mass spectrometry: a review of recent developments, Anal. Chem. 86 (1) (2014) 196–212, doi:10.1021/ac403969n.
[56] Y. Xu, L. Fan, X. Wang, Q. Yong, S.Y. Yu, Simultaneous separation and quantitation of linear xylo- and cello-oligosaccharides mixtures in lignocellulosics processing products on high- performance anion-exchange chromatography coupled with pulsed amperometric detection, Bioresources 8 (3) (2013) 3247–3259, doi:10.15376/biores.8.3.3247-3259.
[57] M. Alyassin, G.M. Campbell, H. Masey O'Neill, M.R. Bedford, Simultaneous determination of cereal monosaccharides, xylo- and arabinoxylo-oligosaccharides and uronic acids using HPAEC-PAD, Food Chem. (2020) 315, doi:10.1016/j.foodchem.2020.126221.
[58] A.G. González, M.Á. Herrador, A practical guide to analytical method validation, including measurement uncertainty and accuracy profiles, TrAC Trends Anal. Chem. 26 (3) (2007) 227–238, doi:10.1016/j.trac.2007.01.009.
[59] G.V. Gautério, T. Hübner, T.R. Ribeiro, A.P.M. Ziotti, S.J. Kalil, Xylooligosaccharide production with low xylose release using crude xylanase from aureobasidium pullulans: effect of the enzymatic hydrolysis parameters, Appl. Biochem. Biotechnol. (2021), doi:10.1007/s12010-021-03658-x.
[60] R. Deutschmann, R.F.H. Dekker, From plant biomass to bio-based chemicals: latest developments in xylan research, Biotechnol. Adv. 30 (6) (2012) 1627–1640, doi:10.1016/j.biotechadv.2012.07.001.
[61] M.G.D. Oliveira, M.B.S. Forte, T.T. Franco, A serial membrane-based process for fractionation of xylooligosaccharides from sugarcane straw hydrolysate, Sep. Purif. Technol. (2022) 278, doi:10.1016/j.seppur.2021.119285.
[62] B. Domon, C.E. Costello, A systematic nomenclature for carbohydrate fragmentations in FAB-MS/MS spectra of glycoconjugates, Glycoconj. J. 5 (4) (1988) 397–409, doi:10.1007/BF01049915.